Evaluations of optical and structural properties of

Co based soft x-ray multilayer gratings

M. Ishino[1], M. Koike[1], F. Satou[2], M. Terauchi[2], K. Sano[3], and H. Sasai[4]

Abstract

The multilayer gratings were fabricated by depositing the Co/Si and Co/SiO$_2$ multilayers onto the surface of laminar-type holographic gratings. The diffraction efficiencies of multilayer gratings were measured at a synchrotron radiation facility, and the structure of Co/Si multilayer grating was observed by a transmission electron microscope. The optical properties evaluated by comparing the measured and calculated incidence and diffraction angles resulted that the diffraction angles of multilayer gratings were affected by the refractive indices of multilayer coatings. The measured low diffraction efficiencies of the Co/Si multilayer grating in the photon energy range of 1–2 keV can be attributed to the inter-diffusion layers with large thickness in the Co/Si multilayer coating.

1 Quantum Beam Science Directorate, Japan Atomic Energy Agency, 8-1, Umemidai, Kizugawa, Kyoto 619-0215, Japan,

2 Institute of Multidisciplinary Research for Advanced Materials, Tohoku University, 2-1-1, Katahira, Aoba-ku, Sendai, Miyagi 980-8577, Japan,

3 Shimadzu Emit, Ltd., 2-5-23, Kitahama, Chuo-ku, Osaka 541-0041, Japan,

4 Consumer and Optical Products Department, Shimadzu Corporation, 1, Nishinokyo-Kuwabaracho, Nakagyo-ku, Kyoto 604-8511, Japan.

1. Introduction

Demand for high throughput spectroscopic instruments for use in the fields of semiconductor devices, catalysts, biomedical observations, and so on, has been increasing. However, current throughput of the spectroscopic instruments, monochromators and spectrometers, employing diffraction gratings with single surface coatings is sometimes not enough to perform in the photon energy range over 2 keV. Also, there has been increasing interest in developing efficient optical dispersive devices effective in a wide photon energy range up to several or 10 keV. A Laminar-type holographic grating with shallow grooves [1] and a blazed grating having a shallow blaze angle [2] demonstrated diffraction efficiency of about 0.1 at the incidence angle of around $\alpha = 89°$ in a photon energy region up to 8 keV. Another approach to improve the diffraction efficiency is the utilization of a multilayer coating [3]. Recently, a laminar-type Co/SiO$_2$ multilayer grating showed the diffraction efficiency of 0.47 at 6.0 keV, and a W/C multilayer grating showed the diffraction efficiency of 0.38 at 8.0 keV [4]. Besides the multilayer coatings mentioned above, Co/Si multilayer was also a candidate for the coating because of its high soft x-ray reflectivity in the calculation [4]. However, it has been reported that Co and Si atoms easily form the inter-diffusion layers with large thickness [5, 6]. The presence of the inter-diffusion layer in a multilayer coating would affect not only on the diffraction efficiency but also on the diffraction condition (incidence and diffraction angles).

In this article, we describe the evaluation of the structural and optical properties of the Co/Si and Co/SiO$_2$ multilayer gratings. The structures of the multilayer gratings were examined by using a transmission electron microscope (TEM). The diffraction conditions of multilayer gratings were measured by an x-ray diffractometer with Cu-$K\alpha$ x rays ($E = 8.05$ keV), and the diffraction efficiencies in the photon energy range of 1–2 keV were measured with the evaluation beam line for soft x-ray optical elements installed on the BL-11 at the SR Center of Ritsumeikan University [7, 8].

2. Fabrication of Multilayer Gratings

Multilayer gratings were fabricated by coating the Co/Si and Co/SiO$_2$ multilayers onto the surfaces of laminar-type holographic gratings. The grating substrates were made of synthetic fused quartz with the size of 40 x 40 mm^2. The surfaces of quartz substrates had the root mean square (rms) roughnesses of $\sigma = 0.36$ nm rms for the Co/Si multilayer grating and of $\sigma = 0.32$ nm rms for the Co/SiO$_2$ multilayer grating. A He/Cd laser ($\lambda = 441.6$ nm) and a photoresist of OFPR5000 were used to make the groove patterns on the substrate surfaces. Then, the patterns were used as masks to rule the laminar-type grooves by reactive ion beam etching using CHF$_3$ gases. Figure 1 shows the surface images of the fabricated laminar-type holographic gratings for (a) Co/Si multilayer grating and for (b) Co/SiO$_2$ multilayer grating observed by an atomic force microscope (AFM), respectively. Both the gratings shown in Figs. 1(a) and 1(b) had the groove density of $1/D = 1200$ lines/mm grooves. The groove depth
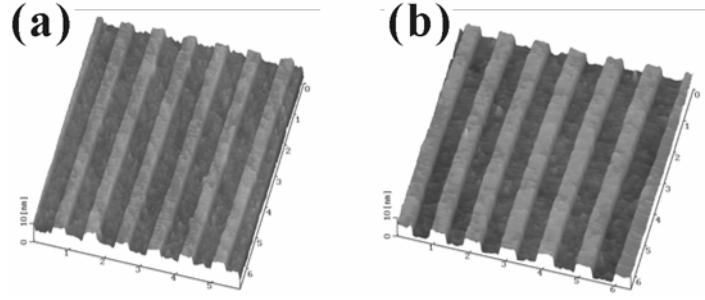
FIG. 1. The AFM images of the fabricated laminar-type holographic gratings for (a) Co/Si multilayer grating and (b) Co/SiO$_2$ multilayer grating. These images were taken before multilayer coatings.

(h) and the land-to-period ratio (a/D) of the grating for the Co/Si multilayer grating were $h = 3.5$ nm and $a/D = 0.40$, where a is the land width of grating groove. For the Co/SiO$_2$ multilayer grating, the grating had the groove depth of $h = 3.5$ nm and the land-to-period ratio of $a/D = 0.34$. The fabrications and evaluations of the laminar-type holographic gratings described above were performed at Shimadzu Corp., Kyoto, Japan.

The Co/Si and the Co/SiO$_2$ multilayers were deposited on the grating surfaces at the Japan Atomic Energy Agency, Kyoto, Japan by means of an ion beam sputtering method. The designed periodic length (d) was intended to be $d = 6.64$ nm [4], which was almost two times of the groove depths of the gratings. The ratio of Co layer thickness (d_{Co}) per periodic length of multilayer ($\Gamma = d_{Co}/d$) was $\Gamma = 0.4$, and the number of multilayer periods was $N = 30$ (60 layers).

Figure 2 shows the x-ray reflectivity curves of the Co/Si and the Co/SiO$_2$ multilayers deposited on the each grating surface. The x-ray reflectivity measurements were carried out in the standard θ–2θ scan mode by use of an x-ray diffractometer at the photon energy of 8.05 keV. To avoid the diffraction peaks from grating grooves, the direction of the grooves was set
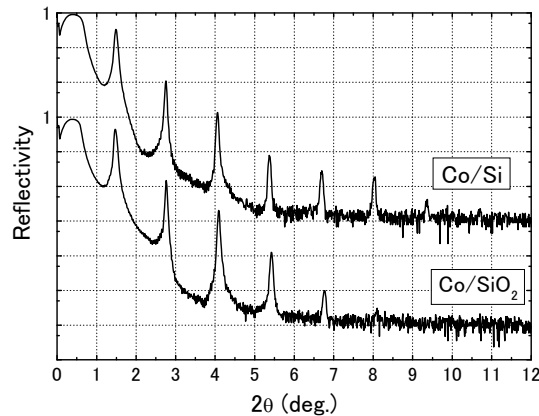
FIG. 2. X-ray reflectivity curves of Co/Si and Co/SiO$_2$ multilayers deposited onto the grating surfaces. The reflectivity curve of Co/SiO$_2$ multilayer was shifted downward for clarity.

to be parallel to the direction of the incident x-rays. The x-ray reflectivity curve of the Co/Si multilayer contains the seven distinct Bragg peaks in the measured 2θ region, and the weak 8th order Bragg peak can be seen around $2\theta = 10.7°$. Similarly, the x-ray reflectivity curve of the Co/SiO$_2$ multilayer also contains the six distinct Bragg peaks. These Bragg peaks appearing clearly in the x-ray reflectivity curves certify the quality of the periodic multilayer structures. The periodic lengths of the deposited multilayers onto the grating surfaces were estimated from the Bragg peak positions appearing in the x-ray reflectivity curves to be $d = 6.63$ nm and 6.56 nm for the Co/Si and Co/SiO$_2$ multilayer gratings, respectively.

3. Results and Discussion

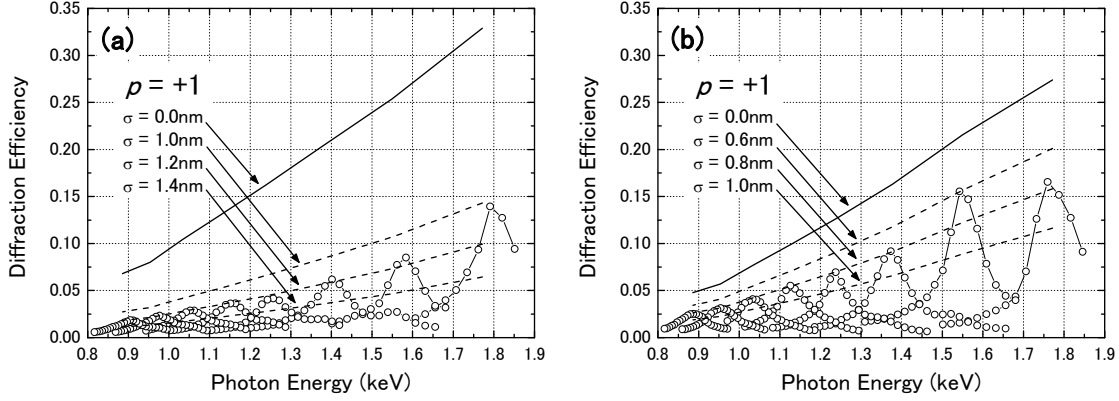### 3.1 Diffraction Efficiencies in $E = 1$–2 keV

The diffraction efficiencies of the Co/Si and Co/SiO$_2$ multilayer gratings in the photon energy range of 1–2 keV were measured at the SR Center of Ritsumeikan University. The diffraction condition (incidence and diffraction angles) of a multilayer grating, where the maximum diffraction efficiency is attained, is described by combining the grating equation and the generalized Bragg's law [9]. The incidence angle (α) is expressed as,

$$\alpha = \sin^{-1}\left[\bar{n} \times \frac{P\left(P^2 + M^2\right) + \sqrt{M^2\left(P^2 + M^2\right)\left[4 - \left(P^2 + M^2\right)\right]}}{2\left(P^2 + M^2\right)}\right], \quad (1)$$

where $\bar{n}$ is the composite average refractive index of multilayer coatings, and P and M are given as,

$$\begin{cases} P = \dfrac{p\lambda}{D} \\ M = \dfrac{m\lambda}{d} \end{cases}, \quad (2)$$

where p and m are the diffraction and reflection order of the grating and the multilayer, respectively [10]. The wavelength of the incident x-ray in the multilayer medium (λ) is related to that in vacuum (λ_0) by $\lambda = \lambda_0/\bar{n}$. It should be noted that, in the actual diffraction efficiency measurement, to obtain the maximum diffraction efficiency, the incidence angle (α) was adjusted around the angle calculated by Eq. (1). Figure 3 shows the measured first-order diffraction efficiencies ($p = +1$) of (a) Co/Si and (b) Co/SiO$_2$ multilayer gratings, shown by symbols (-○-), respectively. The calculated efficiencies ($p = +1$) of the multilayer gratings are also shown as the functions of photon energy (solid lines). The diffraction efficiency calculations were carried out by use of the simulation code, GSOLVER [11]. In the calculation, the periodic lengths of the multilayer coatings on the grating surfaces were chosen to be the values measured by the x-ray diffraction, and the refraction indices were derived from Ref. 12.

FIG. 3. Measured and calculated first-order (p = +1) diffraction efficiencies of (a) Co/Si and (b) Co/SiO$_2$ multilayer gratings in the E = 1–2 keV region. Measured diffraction efficiencies are shown by symbols (-○-) and solid lines are calculated ones assuming ideal structure. Dashed lines describe the calculated efficiencies assuming the Debye-Waller factor.

Assuming that the multilayer gratings have ideal structures (smooth surfaces, abrupt interfaces), the diffraction efficiencies of the Co/Si multilayer grating are expected to be higher than those of the Co/SiO$_2$ multilayer grating (shown as the case of σ = 0.0 nm). However, the measured diffraction efficiencies of the Co/Si multilayer grating were lower than those of the Co/SiO$_2$ multilayer grating in the measured photon energy region. The difference between the calculated and measured efficiencies would be attributed to the imperfect boundaries (such as roughness and inter-diffusion) at the inside of the multilayer coating. To estimate the magnitude of imperfection, we applied the Debye-Waller factor [13],

$$R = R_0 \exp\left[-\left(\frac{4\pi\sigma\cos\alpha}{\lambda_0} \right)^2 \right],$$ (3)

to the diffraction efficiencies. R_0 is the calculated diffraction efficiency assuming an ideal structure (σ = 0.0 nm), and α and λ_0 are the incidence angle and the wavelength of x-rays. σ is the rms roughness including inter-diffusion of the multilayer coating.

In Figs. 3(a) and 3(b), the calculated peak diffraction efficiencies with various rms roughnesses are shown by the dashed lines. The comparison between the calculated diffraction efficiencies assuming the Debye-Waller factor and measured efficiencies suggests that the Co/Si and Co/SiO$_2$ multilayer gratings have rms roughnesses of σ = 1.2 nm rms and σ = 0.8 nm rms, respectively. The estimated roughness of the Co/SiO$_2$ multilayer coating, σ = 0.8 nm rms, is the same with that for the Co/SiO$_2$ multilayer mirror deposited on the Si substrate (σ = 0.8 nm rms) [14]. This value is reasonable with respect to the surface roughness of the grating substrate (σ = 0.32 nm rms). Whereas the surface roughness of the grating substrate for the Co/Si multilayer grating of σ = 0.36 nm rms was almost the same as that of the Co/SiO$_2$ multilayer grating, the estimated roughness of the Co/Si multilayer coating (σ =

1.2 nm rms) was relatively larger than that of the Co/SiO_2 multilayer coating. Because the formation of inter-diffusion layers causes the decrease of optical contrast at the layer boundaries, the imperfect boundary structures not only in roughness but also in inter-diffusion decrease the reflectivity of x-ray multilayer coating.

The measured low diffraction efficiencies and the estimated large rms roughness of the Co/Si multilayer grating would be attributed to the inter-diffusion layers in the Co/Si multilayer coating, because of the Debye-Waller factor including the effect of inter-diffusion.

3.2 TEM Observations

To evaluate the structure of the Co/Si multilayer grating, thin section specimen of the grating was prepared for TEM observations. The observations were carried out by using a
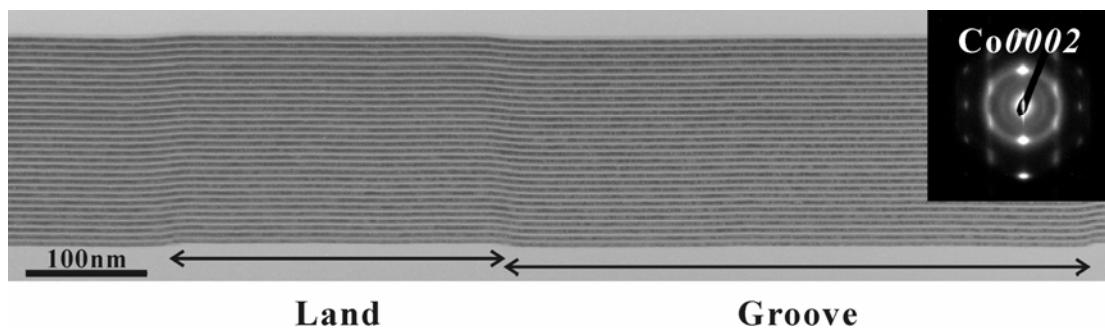
FIG. 4. Cross-sectional TEM image of Co/Si multilayer grating. The SAD pattern is inserted.

JEM2010 TEM at an accelerating voltage of 200 kV. Figure 4 shows the cross-sectional TEM images of Co/Si multilayer grating. The Co layers appear in dark contrast, and Si layers are in light contrast. From the TEM images, it is clear that the Co/Si multilayer grating have the good lateral (grating) and vertical (multilayer coating) structure without serious defects. A selected-area electron diffraction (SAD) pattern obtained from multilayer region is presented as an inset. Circularly distributed intensity in the SAD pattern is assigned to *0002* diffraction intensity of hexagonal Co. The SAD pattern of the Co/Si multilayer coating shows diffraction spots overlapped on the diffraction ring intensity. The spots pattern indicates that crystalline Co particles have preferred orientations with the (*0002*) plane parallel to the grating surface. The preferred orientation of Co crystalline particles was reported for Co/Si multilayers [15] and Co films [16] grown on Si substrates.

Figure 5 shows a high magnification TEM image of the Co/Si multilayer grating. The inter-diffusion layers having an intermediate contrast between the dark contrast (Co) and the light contrast (Si) layers are seen at the interfacial regions. However, the diffraction intensity of Co-silicide, which may be formed in the inter-diffusion layers, was not apparently observed in the SAD pattern. The evaluations of the diffraction efficiency measurement and the TEM observation of the Co/Si multilayer grating indicate that the Co/Si multilayer coating has the large inter-diffusion layers, which degrade the optical performances.
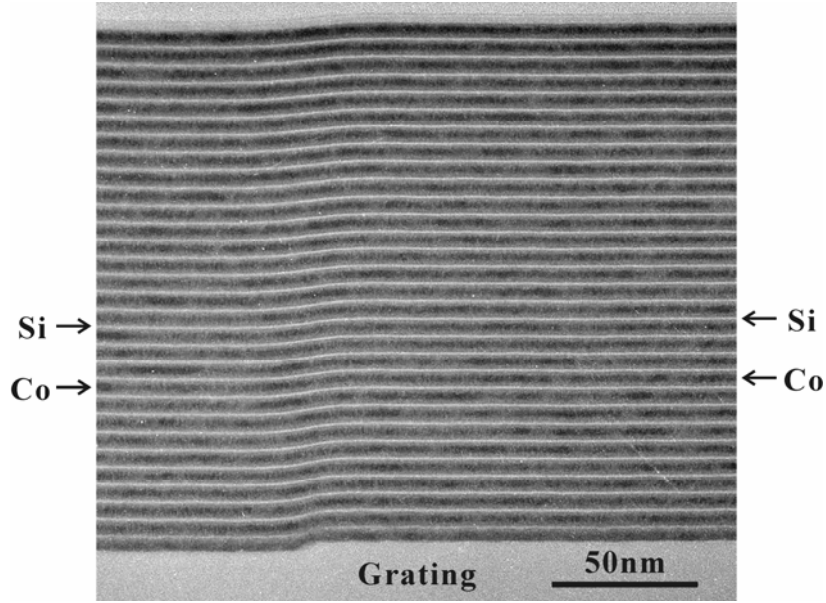
FIG. 5. Cross-sectional TEM image of Co/Si multilayer grating obtained with a high magnification.

3.2 Diffraction Conditions

The diffraction efficiency at the photon energy of 8.05 keV was measured by use of an x-ray diffractometer. Details of the measurement procedure are described in our previous article [4]. Figure 6 shows the measured diffraction efficiencies of (a) Co/Si and (b) Co/SiO_2 multilayer gratings as a function of diffraction angle (β). The diffraction angle is shown as absolute value. The incidence angle (α) and the diffraction orders (p) are indicated in the figures. It is noted that the measured first-order diffraction efficiencies ($p = +1$) of both the Co/Si and Co/SiO_2 multilayer gratings are higher than those of the zeroth-order specular diffraction ($p = 0$), which implies that the Co/Si and Co/SiO_2 multilayer gratings work as the phase gratings. The measured first-order diffraction efficiency of the Co/Si multilayer grating
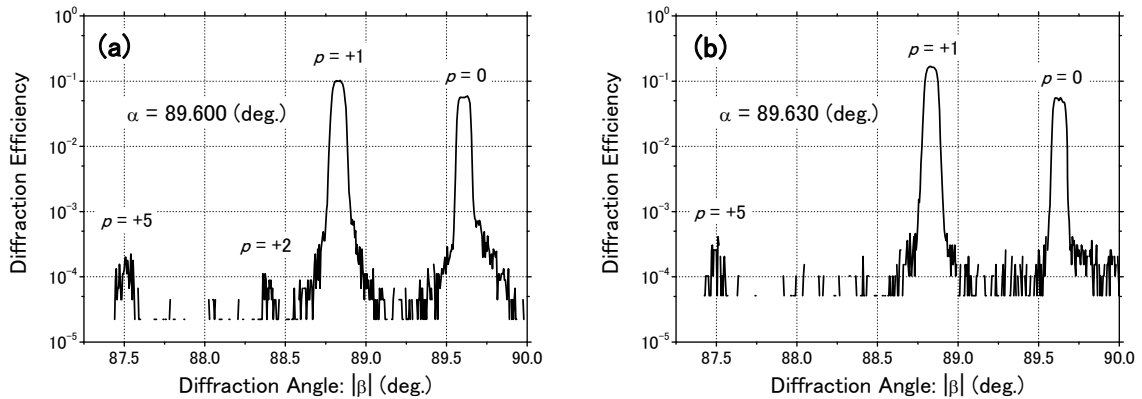
FIG. 6. Measured diffraction efficiencies of (a) Co/Si and (b) Co/SiO_2 multilayer gratings at $E = 8.05$ keV. Abscissa, measured diffraction angle, is shown as absolute value ($|\beta|$) for clarify. α and p in the figures show the measured incidence angle and the diffraction orders.

was 0.100 at the diffraction angle of β = -88.825° [Fig. 6(a)], and that of the Co/SiO$_2$ multilayer grating was 0.168 at β = -88.830° [Fig. 6(b)].

Table I shows the measured and calculated incidence and diffraction angles of the first-order diffraction of the Co/Si and the Co/SiO$_2$ multilayer gratings. The calculations of the diffraction angles were carried out in two different situations; one was the calculation considering the composite averaged refractive index of the multilayer coating ($\bar{n}$), and the other was calculation assuming $\bar{n}$ = 1 for the multilayer coatings. When the composite averaged refractive indices of the multilayer coatings were considered, the values of $\bar{n}$ = 0.9999859 and 0.9999862 were used for the Co/Si and Co/SiO$_2$ multilayer gratings, respectively. The refractive indices of materials were calculated from the tabulated values published by Henke *et al*. [12]. It is obvious that the measured angles of multilayer gratings are closer to the angles calculated using the composite averaged refractive indices of the

TABLE I. Measured and calculated incidence (α) and diffraction (β) angles of the first-order diffraction (p = +1) for the Co/Si and Co/SiO$_2$ multilayer gratings at 8.05 keV. Calculations of angles were carried out in two situations. In one model, the composite averaged refractive indices ($\bar{n}$) of multilayer coatings, $\bar{n}$ = 0.9999859 for the Co/Si multilayer coating and $\bar{n}$ = 0.9999862 for the Co/SiO$_2$ multilayer coating were considered. In the other, the refractive indices of the multilayer coatings were assumed to be $\bar{n}$ = 1.

Multilayer gratings (evaluated periodic length)	Measured angles	Calculated angles	
		$\bar{n}$ = average value	$\bar{n}$ = 1
Co/Si (d = 6.63 nm)	α = 89.600° β = -88.825°	α = 89.631° β = -88.838°	α = 89.790° β = -88.879°
Co/SiO$_2$ (d = 6.56 nm)	α = 89.630° β = -88.830°	α = 89.626° β = -88.837°	α = 89.778° β = -88.876°

multilayer coatings rather than the angles calculated assuming $\bar{n}$ = 1 for the multilayer coatings. This result means that the refractive indices of multilayer coating have to be considered to obtain the maximum efficiency for the multilayer grating.

In the Co/Si multilayer grating, the formations of large inter-diffusion layers has been reported [5, 6]. We have also estimated the structures of the Co/Si multilayer deposited on a Si substrate by use of model fitting calculation for x-ray reflectivity curve at the photon energy of 8.05 keV, and the best-fitted model calculation for the Co/Si multilayer having d = 6.60 nm and Γ = 0.4 suggested that almost of the Si layers are formed into the mixture layers composed of Co and Si atoms [17]. TEM observation of the Co/Si multilayer grating shown in Fig. 5 revealed the existence of the inter-diffusion layers. However, it is difficult to know the phase of the inter-diffusion layer from the TEM image, because the SAD pattern does not

show the diffraction intensity of Co-silicide particles (shown in Fig. 4).

The phase of the inter-diffusion layers can be estimated from the calculation of the incidence and diffraction angles of the Co/Si multilayer grating because these angles are affected by the refractive indices of multilayer coatings. Co-silicide compounds have three phases of Co_2Si, $CoSi$, and $CoSi_2$. Calculations for the multilayer gratings assuming these three compound layers, i.e., $Co/Co_2Si/Si$, $Co/CoSi/Si$, and $Co/CoSi_2/Si$ multilayer coatings, were carried out. The periodic lengths of the multilayer coating was $d = 6.63$ nm, which was the same with that of the Co/Si multilayer coating. The thickness of the light contrast layer supposed to be Si layer in Fig. 5 is about 0.6 nm, which is the same with the estimated Si layer thicknesses from the model calculation [17]. The thicknesses of Co and Si layers in the multilayer coatings were $d_{Co} = 2.65$ nm and $d_{Si} = 0.60$ nm, respectively, so that those of compound layers were calculated to be 3.38 nm. Table II shows the calculated angles of the first-order diffraction for the multilayer gratings. The calculation for the Co/(Co + Si)/Si multilayer coating assuming a mixture of equal amounts of Co and Si is also listed in Table II.

TABLE II. Calculated incidence (α) and diffraction (β) angles of the first-order diffraction ($p = +1$) for the $Co/Co_2Si/Si$, $Co/CoSi/Si$, $Co/CoSi_2/Si$ multilayer gratings at 8.05 keV. Calculated angles of the Co/(Co + Si)/Si multilayer grating assuming the mixture layer is also listed. $\bar{n}$ in the table represents the composite averaged refractive indices of multilayer coatings.

Assumed multilayer coatings (Average refractive indicies)	Calculated angles	Measured angles (Co/Si multilayer grating)
$Co/Co_2Si/Si$ ($\bar{n} = 0.9999793$)	$\alpha = 89.576°$ $\beta = -88.820°$	$\alpha = 89.600°$ $\beta = -88.825°$
$Co/CoSi/Si$ ($\bar{n} = 0.9999801$)	$\alpha = 89.582°$ $\beta = -88.822°$	
$Co/CoSi_2/Si$ ($\bar{n} = 0.9999822$)	$\alpha = 89.599°$ $\beta = -88.828°$	
$Co/(Co + Si)/Si$ ($\bar{n} = 0.9999818$)	$\alpha = 89.595°$ $\beta = -88.827°$	

Among the multilayer gratings listed in Table II, the calculated angles of the $Co/CoSi_2/Si$ and Co/(Co + Si)/Si multilayer gratings are almost the same as the measured angles. The phase of the inter-diffusion layers was estimated to be $CoSi_2$ nano particles and/or a mixture of Co and Si from the calculation. This result also indicates that the Co/Si multilayer coating on the grating surface has large inter-diffusion layers.

4. Conclusion

The structural and optical properties of Co/Si and Co/SiO_2 multilayer gratings were evaluated. The diffraction efficiencies of Co/Si and Co/SiO_2 multilayer gratings in the 1–2

keV range were measured, and they were compared with calculations assuming the imperfect boundaries. TEM observations showed that inter-diffusion layers were found at the interfaces of the Co and Si layers in the Co/Si multilayer coating. From the comparisons between measured and calculated diffraction conditions (incidence and diffraction angles) of multilayer gratings, it was concluded that the refractive indices of the multilayer coating have to be considered for obtaining the maximum efficiency, because the incidence and diffraction angles considering the refractive indices were significantly different from angles assuming the refractive indices of unity even at 8.05 keV.

It is concluded that the large apparent roughness of the Co/Si multilayer grating can be attributed to the inter-diffusion layers in the multilayer coating. The combination of Co and Si in a multilayer structure is thus concluded to be unfavorable for a multilayer structure for use as an x-ray optical coating. On the other hand, the Co/SiO_2 multilayer is a quite appropriate system for optical elements such as grating and mirror for use in a wide photon energy range up to several or 10 keV.

References

[1] P. A. Heimann, M. Koike, and H. A. Padmore, Rev. Sci. Instrum. **76**, 063102 (2005).

[2] D. Cocco, A. Bianco, B. Kaulich, F. Schaefers, M. Mertin, G. Reichardt, B. Nelles, and K. F. Heidemann, AIP Conf. Proc. **879**, 497–500 (2007).

[3] T. W. Barbee, Jr., Rev. Sci. Instrum. **60**, 1588–1595 (1989).

[4] M. Ishino, P. A. Heimann, H. Sasai, M. Hatayama, H. Takenaka, K. Sano, E. M. Gullikson, and M. Koike, Appl. Opt. **45**, 6741–6745 (2006).

[5] P. Ruterana, P. Houdy, and P. Boher, J. Appl. Phys. **68**, 1033–1037 (1990).

[6] J. M. Fallon, C. A. Faunce, and P. J. Grundy, J. Appl. Phys. **88**, 2400–2407 (2000).

[7] M. Koike, K. Sano, O. Yoda, Y. Harada, M. Ishino, N. Moriya, H. Sasai, H. Takenaka, E. Gullikson, S. Mrowka, M. Jinno, Y. Ueno, J. H. Underwood, and T. Namioka, Rev. Sci. Instrum. **73**, 1541–1544 (2002).

[8] M. Koike, K. Sano, Y. Harada, O. Yoda, M. Ishino, K. Tamura, K. Yamashita, N. Moriya, H. Sasai, M. Jinno, and T. Namioka, Proc. SPIE **4782**, 300–307 (2002).

[9] W. K. Warburton, Nucl. Instrum. Methods Phys. Res. A **291**, 278–285 (1990).

[10] K. Krastev, F. LeGuern, K. Coat, R. Barchewitz, J-M. Andre, M. F. Ravet, E. Cambril, F.

Rousseaux, and P. Davi, Nucl. Instrum. Methods A **368**, 533–542 (1996).

[11] GSOLVER V4.2b, Grating Solver Development Co., Allen, Texas.

[12] B. L. Henke, E. M. Gullikson, and J. C. Davis, At. Data Nucl. Data Tables **54**, 181–342 (1993).

[13] E. Spiller, "*Soft X-ray Optics*", SPIE Optical Engineering Press (1994).

[14] M. Ishino, M. Koike, M. Kanehira, F. Satou, M. Terauchi, and K. Sano, J. Appl. Phys. **102**, 023513 (2007).

[15] A. Jaiswal, S. Rai, M. K. Tiwari, V. R. Reddy, G. S. Londha, and R. V. Nandedkar, J. Phys.: Condens. Matter **19**, 016001 (2007).

[16] A. Kharmouche, S-M. Cherif, A. Bourzami, A. Layadi, and G. Schmerber, J. Phys. D: Appl. Phys. **37**, 2583–2587 (2004).

[17] M. Ishino, M. Koike, K. Sano, and E. M. Gullikson, JAEA-Conf **2007-001**, 225-228 (2007), (in Japanese).